INSTITUTE OF PHYSICS PUBLISHING JOURNAL OF PHYSICS D: APPLIED PHYSICS

J. Phys. D: Appl. Phys. **37** (2004) 326–333 PII: S0022-3727(04)62213-3

Effects of lossy, layered filler particles on the bulk permittivity of a composite material

N Bowler[1]

Center for Nondestructive Evaluation, Iowa State University, Applied Sciences Complex II, Ames, IA 50011, USA

E-mail: nicolabowler@ieee.org

Received 15 April 2003
Published 14 January 2004
Online at stacks.iop.org/JPhysD/37/326 (DOI: 10.1088/0022-3727/37/3/003)

Abstract

The ability to control the frequency at which a dielectric material exhibits maximum loss (the relaxation frequency) is of interest in telecommunications and radar absorption. A theoretical investigation of the behaviour of the complex bulk permittivity of a composite material with coated, spheroidal filler particles is presented. In the model, the filler particles are replaced mathematically by electric multipole sources located at their centres (Harfield N 2000 *J. Mater. Sci.* **35** 5809–16). It is shown how factors such as particle shape, orientation with respect to the applied electric field, thickness of coating and permittivity value of the individual phases influences the bulk permittivity of the composite material. For a composite with coated filler particles, one or two relaxation frequencies may be observed. Employing the theory of Pauly and Schwan (Hanai T 1968 Electrical properties of emulsions *Emulsion Science* ed P Sherman (London: Academic)), particular attention is paid to the way in which the relaxation frequencies are affected by the material parameters.

1. Introduction

The dielectric dispersion characteristics of a composite material can be controlled by adjusting the material parameters of the individual phases. In a composite with coated filler particles, these parameters are the particle volume fraction, shape, orientation and layer thickness, and the permittivity values of the phases. Of particular interest in telecommunications and radar absorption is the frequency at which a material exhibits maximum loss, and the magnitude of that loss. A systematic study, of the relaxation processes which occur in a material composed of coated filler particles dispersed in a matrix, is presented here. Indications are given as to how to achieve maximum absorption at a chosen frequency.

This study is based on two models of the bulk permittivity of a composite material. The first assumes that the particles are sufficiently well separated that the electric potential in the neighbourhood of any one particle is not influenced by the presence of the others [1]. The precise spatial arrangement of the particles is not important. The analysis results in closed-form expressions for the bulk permittivity of the material, $\epsilon(\omega)$, and for the frequencies at which relaxation occurs, ν_1 and ν_2. The second model accounts for perturbation of the electric potential in the vicinity of a particle, due to its neighbours, by arranging the particles on a simple-cubic lattice and describing them mathematically as electric multipole source distributions [2]. This leads to greater accuracy in the result for ϵ, expressed as a truncated series expansion, although complexity of the expressions prohibits obtaining explicit forms for ν_1 and ν_2. The first model is for spherical filler particles whereas the second can be applied also in the case of spheroidal particles.

[1] Formerly N Harfield.

2. Theory for spherical filler particles

Consider a time-harmonic electric field, $\boldsymbol{E} = E_0 \exp(-\mathrm{i}\omega t)$, where $\omega = 2\pi\nu$ is the angular frequency of the excitation, ν being the frequency measured in hertz. The constitutive relation connecting the electric field and the electric flux

density, $\boldsymbol{D}$, is

$$\boldsymbol{D} = \epsilon_0 \epsilon_j' \boldsymbol{E}, \tag{1}$$

where ϵ_j' (real) is the permittivity of the jth medium, relative to the permittivity of free space $\epsilon_0 = 8.85 \times 10^{-12}\,\mathrm{F\,m^{-1}}$. The Maxwell–Ampère law, combined with the constitutive relation (1), suggests defining a complex permittivity

$$\epsilon_j = \epsilon_j' + \mathrm{i}\epsilon_j'' \qquad \text{with } \epsilon_j'' = \frac{\sigma_j}{\omega\epsilon_0}, \tag{2}$$

where σ_j is the conductivity of the medium.

In this section, two methods are summarized, by which the bulk complex permittivity of a composite with coated, spherical filler particles may be calculated. The first is due to Pauly and Schwan [1] and treats the system as a dilute mixture of dispersed particles. Closed-form expressions for the bulk permittivity of the system, $\epsilon(\omega)$, and the relaxation frequencies, ν_1 and ν_2, are obtained. The second method treats the particles mathematically as electric multipole sources [2]. This means that higher order interactions between the filler particles are accounted for. The resulting expression for $\epsilon(\omega)$ is more accurate, and naturally more complicated, than that obtained by Pauly and Schwan. Explicit expressions for the ν_k are not obtained in this model due to the prohibitive complexity of the analysis.

2.1. Dipole model

In this summary of the theory due to Pauly and Schwan [1], the development as laid out by Hanai [3] is followed. First, the electric potential, exterior to one filler particle in a uniform electric field, is written down according to potential theory of the electric field. Then the potential exterior to a spherical region of radius D, containing a collection of N dispersed filler particles, is written down by superposition of the potentials due to the individual particles. The expression for the potential is a function of the permittivity values, ϵ_j, and volume fractions, f_j, of the individual phases, $j = 1, 2, 3$, as shown in figure 1. It is implicit in this model that the particles do not interact.

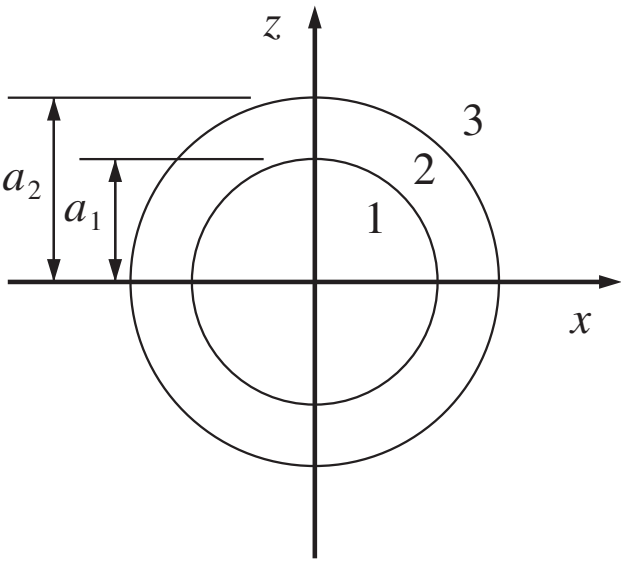

Figure 1. Cross-section of a coated sphere.

The potential exterior to the collection of N particles is then equated with that due to a sphere of radius D with bulk permittivity ϵ. Thus, an expression for ϵ is obtained in terms of the permittivities and volume fractions of the individual phases:

$$\begin{aligned}\frac{\epsilon}{\epsilon_3} = 1 + 3\,[&f(\epsilon_1 + 2\epsilon_2)(\epsilon_2 - \epsilon_3) + f_1(\epsilon_1 - \epsilon_2)(2\epsilon_2 + \epsilon_3)] \\ &\times\left[(\epsilon_1 + 2\epsilon_2)(\epsilon_2 + 2\epsilon_3) + 2\left(\frac{f_1}{f}\right)(\epsilon_1 - \epsilon_2)(\epsilon_2 - \epsilon_3)\right. \\ &\left. - f(\epsilon_1 + 2\epsilon_2)(\epsilon_2 - \epsilon_3) - f_1(\epsilon_1 - \epsilon_2)(2\epsilon_2 + \epsilon_3)\right]^{-1}.\end{aligned} \tag{3}$$

Here, $f = f_1 + f_2$ is the volume fraction of the whole particle (core and layer together). Equation (3) is identical to that obtained by Sihvola and Lindell [4] for a three-phase mixture. Hanai shows how equation (3) may be rearranged to reveal two Debye-type dispersions,

$$\epsilon = \epsilon_\infty' + \frac{\epsilon'(0) - \epsilon_i'}{1 - \mathrm{i}\omega\tau_1} + \frac{\epsilon_i' - \epsilon_\infty'}{1 - \mathrm{i}\omega\tau_2} + \mathrm{i}\epsilon''(0), \tag{4}$$

occurring at frequencies $\nu_k = 1/(2\pi\tau_k)$, $k = 1, 2$. In equation (4), $\epsilon_\infty' = \lim_{\omega\to\infty}(\epsilon)$ and ϵ_i' is a permittivity value intermediate between $\epsilon'(0)$ and ϵ_∞' at which $\epsilon'(\omega)$ may plateau between the two relaxation processes. Closed-form expressions for the terms in equation (4) are given as functions of the material parameters in [3]. Of particular interest in this paper is the way in which the relaxation frequencies depend on the parameters of the system, so equations for the ν_k are reproduced in the appendix.

2.2. Multipole model

Following the method of Zuzovsky and Brenner [5] and Sangani and Yao [6], the bulk permittivity of a composite material can be obtained for closely approaching, coated particles by treating them as multipole source distributions located at their centres [2]. In order to account for interactions between the filler particles, they are arranged on the sites of a simple-cubic lattice. This permits the electric potential to be expressed as a periodic, singular solution of Laplace's equation. The potential in this form is then matched with an expression for the potential exterior to one representative coated particle, and the following expression for ϵ obtained in terms of the parameters of the system.

$$\frac{\epsilon}{\epsilon_3} = 1 - 3f\left[\frac{1}{\mathcal{L}_1^{23}} + f + c_1 f^{10/3} + c_2 f^{14/3} + \mathcal{O}(f^{18/3})\right]^{-1}. \tag{5}$$

The series has been truncated at a point where, to obtain further terms, the mathematical analysis becomes prohibitively lengthy. The method lends itself to numerical generalization, however, where greater accuracy could be obtained. In equation (5), the c_i are given by

$$c_1 = -\frac{16(3/4\pi)^{10/3}(a_{20}')^2}{1/\mathcal{L}_3^{23} + 20(3/4\pi)^{7/3}a_{30}' f^{7/3}}, \tag{6}$$

$$c_2 = -176\left(\frac{3}{4\pi}\right)^{14/3}\mathcal{L}_5^{23}(a_{30}')^2, \tag{7}$$

where $\mathcal{L}_s^{23}$ is a coefficient obtained by applying continuity conditions on the electric potential at the surface of the filler particles.

$$\mathcal{L}_s^{23} = \frac{1 - \rho_{23} g_s}{\rho_{23} g_s + (s+1)/s}, \tag{8}$$

wherein

$$\rho_{ij} = \frac{\epsilon_i}{\epsilon_j}, \tag{9}$$

$$g_s = \frac{1 - [(s+1)/s](f_1/f)^{(2s+1)/3} \mathcal{L}_s^{12}}{1 + (f_1/f)^{(2s+1)/3} \mathcal{L}_s^{12}} \tag{10}$$

and $\mathcal{L}_s^{12}$ is a coefficient obtained by applying continuity conditions on the electric potential at the interface between the core and layer of the filler particles; regions 1 and 2.

$$\mathcal{L}_s^{12} = \frac{1 - \rho_{12}}{\rho_{12} + (s+1)/s}. \tag{11}$$

The coefficients $a'_{nm} = l^{2n+1} a_{nm}$, where l is the side length of the unit cell of the simple-cubic lattice, arise in summing over an infinite number of lattice sites and have numeric value [6]

$$a_{20} = 3.108\,227, \qquad a_{30} = 0.573\,329\,3.$$

Equation (5) reduces to equation (3) if only the first two terms in the series, $(\mathcal{L}_1^{23})^{-1} + f$, on the right-hand side of (5) are retained.

3. Example calculations for spherical filler particles with a lossy core

Consider a composite material in which the coated filler particles have a core which is lossy dielectric (complex permittivity). If the particle coating is lossless, one relaxation process is observed. It is associated with the entrapment of free charges, found in the core, at the core-layer interface. This is an example of interfacial polarization. If the coating is lossy, the situation is more complicated and two relaxation processes may be observed depending on the relative values of the complex permittivity in the core and surface layer of the filler particle.

These effects are investigated systematically here by using theoretical models described above. Results from the closed-form expressions for the relaxation frequencies, yielded by the dipole model, are shown to agree quite well in many cases with results calculated using the multipole model.

In this investigation, the matrix is assigned the material properties of free space, $\epsilon_3 = 1 + \mathrm{i}0$, since the focus is on the role of the filler particles in determining the bulk permittivity of the composite, ϵ. All quoted permittivity values are relative to the permittivity of free space, $\epsilon_0 = 8.85 \times 10^{-12}\,\mathrm{F\,m^{-1}}$.

3.1. Lossless layer

In figure 2, the calculated bulk permittivity is shown for a material with filler particles whose layer is lossless and whose core is lossy. The particle volume fraction, f, is 0.4 and

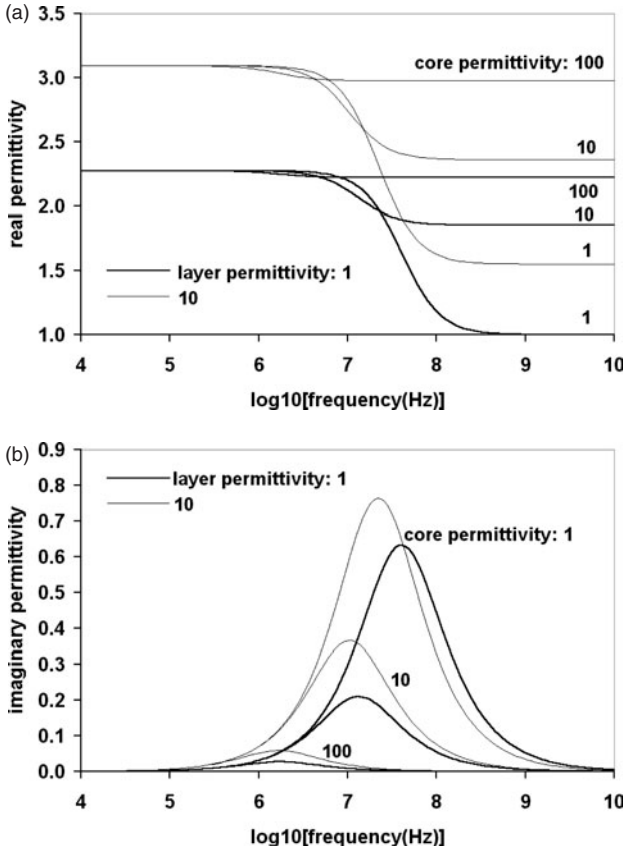

Figure 2. Bulk permittivity ϵ as a function of frequency, ν. The particle core is lossy dielectric with $\epsilon'_1 = 1$, 10 or 100 and $\sigma_1 = 0.01\,\mathrm{S\,m^{-1}}$. The particle layer is lossless with $\epsilon'_2 = 1$ or 10. All permittivity values are relative to the permittivity of free space, $\epsilon_0 = 8.85 \times 10^{-12}\,\mathrm{F\,m^{-1}}$. The particle volume fraction, f, is 0.4 and the layer thickness is 10% of the particle radius, denoted $t = 0.1$.

the normalized layer thickness $t = 0.1$ where, employing the notation of figure 1,

$$t = \frac{a_2 - a_1}{a_2}. \tag{12}$$

The real permittivity of the layer is assigned values $\epsilon'_2 = 1$ and 10. The real permittivity of the core takes values $\epsilon'_1 = 1$, 10 and 100 and the conductivity of the core, σ_1, is $0.01\,\mathrm{S\,m^{-1}}$.

It can be seen, from figure 2, that the low-frequency limiting permittivity value, $\epsilon(0)$, changes as a function of ϵ'_2. This contrasts with results for the converse case in which the layer is lossy and the core is lossless [7]. It remains true that, in the lossy phase, the imaginary part of the complex permittivity is much larger than the real part at low-frequency but here ϵ'_2 plays a significant role in determining $\epsilon(0)$ because of its prominent location at the exterior of the filler particles. Previously, in the case of a lossy layer and lossless core, the imaginary part of the layer permittivity dominated at low-frequency and variations in ϵ'_2 and ϵ'_1 did not result in a change in $\epsilon(0)$. The high-frequency limiting value of bulk permittivity seen in figure 2 is governed by both ϵ'_1 and ϵ'_2.

Figure 2(*b*) shows that, as the real core permittivity increases, the loss peak reduces in magnitude and shifts to lower frequency. If the real permittivity of the layer increases,

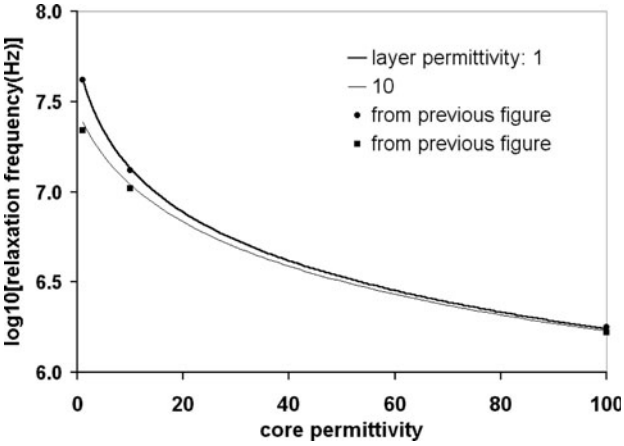

Figure 3. Relaxation frequency as a function of ϵ_1' and ϵ_2'. Other parameters are as in figure 2. Relaxation frequencies from figure 2 are also plotted.

the family of curves, obtained by changing ϵ_1', also shifts to lower frequency but the loss peaks increase in magnitude.

The way in which the relaxation frequency varies as a function of ϵ_1', for $\epsilon_2' = 1$ and 10, is shown in figure 3. All other parameters are as shown in figure 2. These curves are calculated by means of equation (19), derived from treating the filler particles as dipole sources in the applied electric field. In this case of a lossy core and lossless layer, only one relaxation process is observed, with frequency ν_2. The relaxation frequency is highest for $\epsilon_1' = 1$, declining as ϵ_1' increases. ν_2 also declines as ϵ_2' increases.

The three values of relaxation frequency seen in figure 2 and calculated using the multipole model are also plotted. The results of the dipole and multipole models agree better for $\epsilon_2' = 1$ than for $\epsilon_2' = 10$. For $\epsilon_1' = 1$, the discrepancies are roughly 2% and 12%, respectively. This is to be expected since there are stronger variations in the electric potential near the particles when the dielectric contrast between the phases is higher, and these variations are more accurately described by the multipole model.

3.2. Lossy layer

3.2.1. Effect of σ_1. In figure 4, the bulk permittivity is shown for a composite material with filler particles whose core and layer are both lossy. σ_2 is fixed at 0.01 S m^{-1} while σ_1 takes several values, as indicated, and $\epsilon_1' = \epsilon_2' = 1$. $f = 0.4$ and $t = 0.1$. When the core and layer both have the same conductivity, there is a single loss process since the particle is homogeneous. As the core conductivity increases, a second loss peak emerges and moves to increasingly higher frequency. This indicates that ν_2 is strongly influenced by σ_1, when $\sigma_1 \gg \sigma_2$.

The way in which ν_1 and ν_2 depend on σ_1 is shown for this case in figure 5. It can be seen how, when $\sigma_1/\sigma_2 \gg 1$, ν_1 becomes independent of σ_1, tending to a constant value, whereas $\nu_2 \propto \sigma_1$. Hence, as $\sigma_1/\sigma_2 \to \infty$, the frequency separation between the loss peaks increases. When $\sigma_1/\sigma_2 \ll 1$, both ν_1 and ν_2 tend to constant values, independent of σ_1. The loss peak associated with ν_2 is negligible in magnitude compared with that at ν_1 however, for $\sigma_1/\sigma_2 \leqslant 1$, so, practically speaking, only ν_1 is important in this regime.

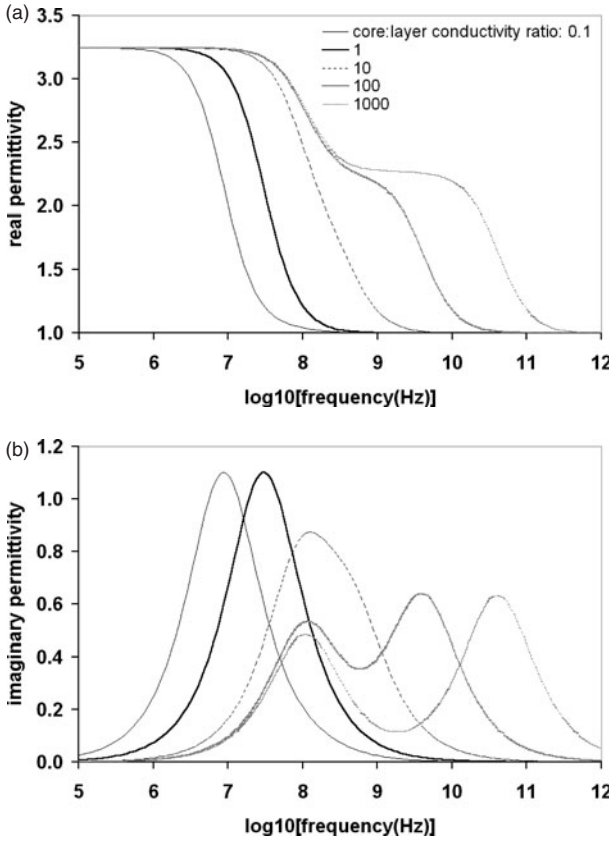

Figure 4. ϵ as a function of ν and σ_1. $\epsilon_1' = 1$ and σ_1 takes a variety of values, as indicated. $\epsilon_2' = 1$ and $\sigma_2 = 0.01$ S m^{-1}. $f = 0.4$ and $t = 0.1$.

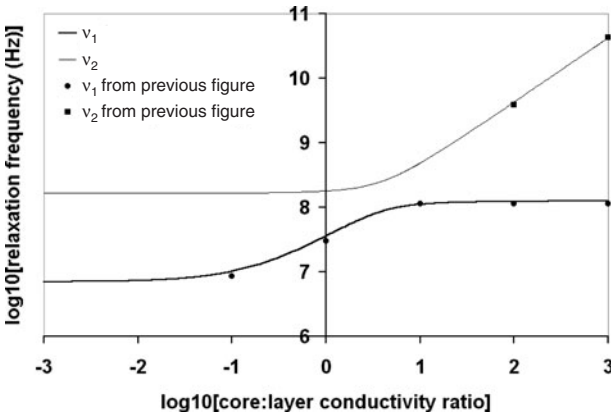

Figure 5. Relaxation frequencies ν_1 and ν_2 as functions of σ_1. $\sigma_2 = 0.01$ S m^{-1} and other parameters are as in figure 4. Values of ν_1 and ν_2 obtained from figure 4 (multipole model) are also shown.

3.2.2. Effect of σ_2. Now observe the effect of holding σ_1 fixed at 0.01 S m^{-1} and varying σ_2, figure 6. Other parameters remain as shown in figure 4. As the layer conductivity decreases, ν_1 moves to increasingly lower frequency. This indicates that ν_1 is strongly influenced by σ_2, when $\sigma_2 \ll \sigma_1$. The way in which the relaxation frequencies depend on σ_2 is shown in figure 7. ν_1 is observed to be proportional to σ_2 for both $\sigma_2/\sigma_1 \ll 1$ and $\gg 1$, with a nonlinear region between the asymptotes. ν_2 becomes independent of σ_2 as $\sigma_2/\sigma_1 \to 0$. For $\sigma_2/\sigma_1 \to \infty$, ν_2 is shown in figure 7 to be proportional to σ_2,

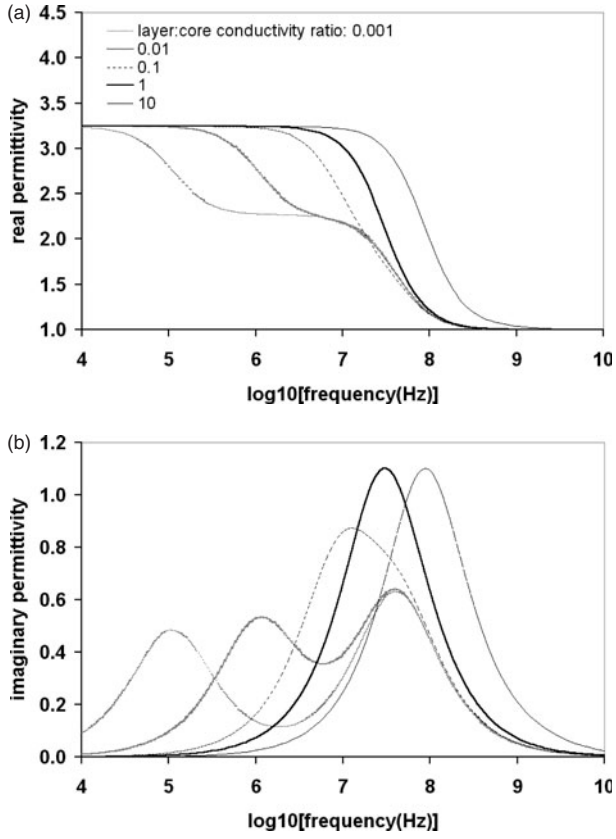

Figure 6. ϵ as a function of ν and σ_2. $\epsilon_1' = \epsilon_2' = 1$. $\sigma_1 = 0.01\,\mathrm{S\,m^{-1}}$ and σ_2 takes a variety of values, as indicated. $f = 0.4$ and $t = 0.1$.

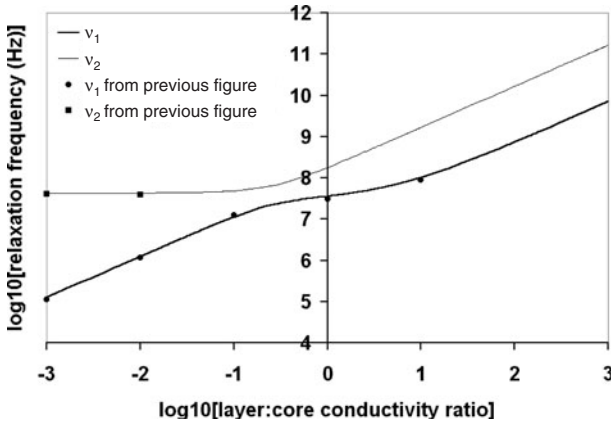

Figure 7. Relaxation frequencies ν_1 and ν_2 as functions of σ_2. $\sigma_1 = 0.01\,\mathrm{S\,m^{-1}}$ and other parameters are as in figure 6. Values of ν_1 and ν_2 obtained from figure 6 (multipole model) are also shown.

but in practice, the magnitude of the loss process is negligible compared with that at ν_1 in this regime.

By comparing the results of figures 4 and 6, it can be seen that, if the ratio σ_1/σ_2 is maintained while σ_1 and σ_2 vary, the curves describing the $\epsilon(\nu)$ preserve their shape but shift in frequency in proportion to the change in conductivity. This point is discussed in [7].

3.2.3. Effect of ϵ_1'. In figure 8, the case in which $\sigma_1 = 1.0\,\mathrm{S\,m^{-1}}$, shown in figure 4, is taken and the real permittivity of the particle core is varied. It is clear that $\epsilon(0)$,

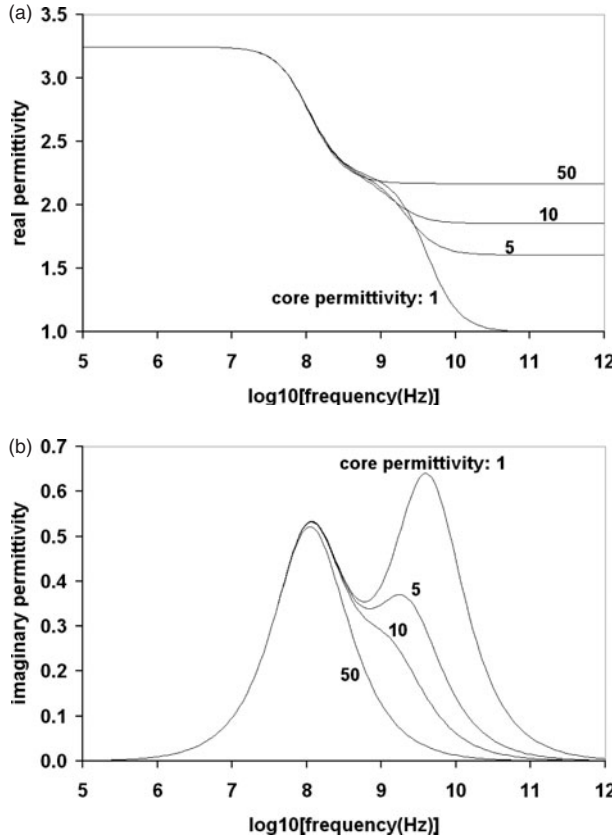

Figure 8. ϵ as a function of ν and ϵ_1'. ϵ_1' takes a variety of values, as indicated, and $\sigma_1 = 1.0\,\mathrm{S\,m^{-1}}$. $\epsilon_2' = 1$ and $\sigma_2 = 0.01\,\mathrm{S\,m^{-1}}$. $f = 0.4$ and $t = 0.1$.

ϵ_i and the low-frequency loss process are largely unaffected by adjusting ϵ_1', whereas the effect on ϵ_∞ is strong. This is due to the fact that, in the high-frequency regime, the imaginary part of the complex permittivity becomes small, being inversely proportional to ν, and hence ϵ_∞ is governed by ϵ_1' and ϵ_2'. As ϵ_1' increases, the magnitude of the higher frequency loss process declines until eventually it is negligible in comparison with that at ν_1.

3.2.4. Effect of ϵ_2'. In figure 9, the real permittivity of the particle layer is varied for the case in which $\sigma_1 = 1.0\,\mathrm{S\,m^{-1}}$, shown in figure 4. Both ϵ_i and ϵ_∞ are strongly affected by adjusting ϵ_2'.

3.2.5. Effect of t. The bulk permittivity of a composite with filler particles whose core and layer are both lossy is shown as a function of layer thickness in figure 10. $f = 0.4$, $\sigma_1 = 1.0\,\mathrm{S\,m^{-1}}$, $\sigma_2 = 0.01\,\mathrm{S\,m^{-1}}$ and $\epsilon_1' = \epsilon_2' = 1$. In the case of no layer ($t = 0$) or full-thickness layer ($t = 1$) a single loss peak is observed since the filler particles are then homogeneous. For intermediate values of t, two loss peaks are seen, demonstrating the presence of constituent materials with different values of conductivity.

4. Multipole theory for spheroidal filler particles

Consider a composite with coated, spheroidal filler particles located at the nodes of a simple-cubic lattice. One

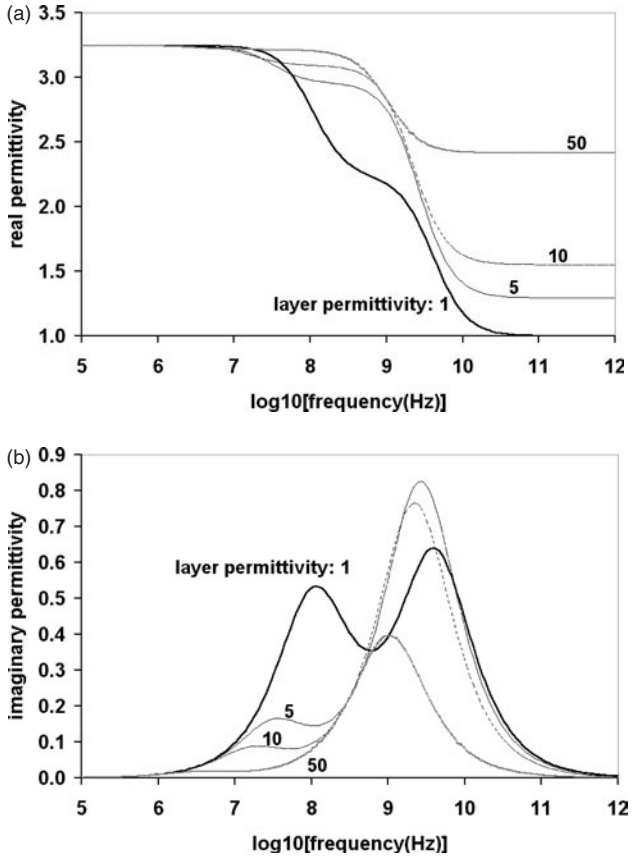

Figure 9. ϵ as a function of ν and ϵ_2'. $\epsilon_1' = 1$ and $\sigma_1 = 1.0\,\mathrm{S\,m^{-1}}$. ϵ_2' takes a variety of values, as indicated, and $\sigma_2 = 0.01\,\mathrm{S\,m^{-1}}$. $f = 0.4$ and $t = 0.1$.

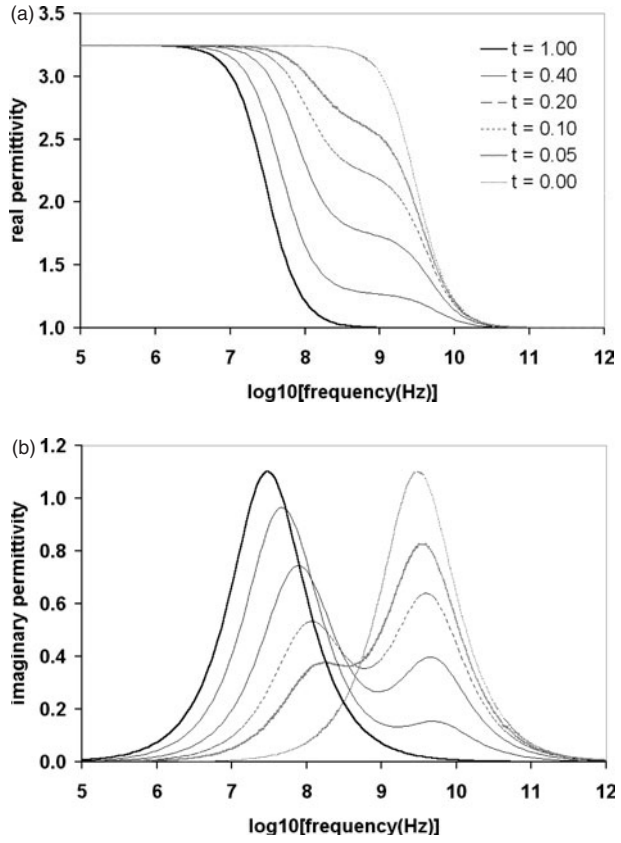

Figure 10. ϵ as a function of ν and t. $\epsilon_1' = \epsilon_2' = 1$, $\sigma_1 = 1.0\,\mathrm{S\,m^{-1}}$ and $\sigma_2 = 0.01\,\mathrm{S\,m^{-1}}$. $f = 0.4$.

representative filler particle is shown in figure 11. The particles are aligned with one another and with one of the lattice vectors, leading to anisotropy in the bulk permittivity, now a second-order tensor with two independent components ϵ_{xx} $(=\epsilon_{yy})$ and ϵ_{zz}. Following the mathematical method describing a similar composite with spherical filler particles, outlined in section 2.2, expressions for ϵ_{xx} and ϵ_{zz} may be obtained by suitably transforming the multipole expansion for the electric potential, previously written in terms of spherical harmonics, into spheroidal harmonics. This periodic, singular solution of Laplace's equation is then matched with an expression for the potential exterior to a representative filler particle, derived from potential theory of the electric field, also written in terms of spheroidal harmonics. Details are given in [2, 9]. The following expressions for ϵ_{xx} and ϵ_{zz} are obtained

$$\frac{\epsilon_{xx}}{\epsilon_3} = 1 - 4\pi\lambda^3\left[-\frac{3}{2\mathcal{L}_{11}^{23}} + \frac{4\pi}{3}\lambda^3 + \mathcal{O}(\lambda^5)\right]^{-1}, \quad (13)$$

$$\frac{\epsilon_{zz}}{\epsilon_3} = 1 - 4\pi\lambda^3\left[\frac{3}{\mathcal{L}_{10}^{23}} + \frac{4\pi}{3}\lambda^3 + \mathcal{O}(\lambda^5)\right]^{-1}. \quad (14)$$

In the above expressions, $\lambda = d/l$, where $2d$ is the interfocal length of the spheroid, and $\mathcal{L}_{\mathrm{st}}^{23}$ is a coefficient obtained by applying continuity conditions on the electric field at the surface of the filler particles:

$$\mathcal{L}_{\mathrm{st}}^{23} = [(1-\rho_{23})P_s^t(\xi_2)P_s^t(\xi_2)' + \mathcal{L}_{\mathrm{st}}^{12}[P_s^t(\xi_2)'Q_s^t(\xi_2) - \rho_{23}P_s^t(\xi_2)Q_s^t(\xi_2)']][\rho_{23}P_s^t(\xi_2)'Q_s^t(\xi_2) - P_s^t(\xi_2)Q_s^t(\xi_2)' + \mathcal{L}_{\mathrm{st}}^{12}(\rho_{23}-1)Q_s^t(\xi_2)Q_s^t(\xi_2)']^{-1}. \quad (15)$$

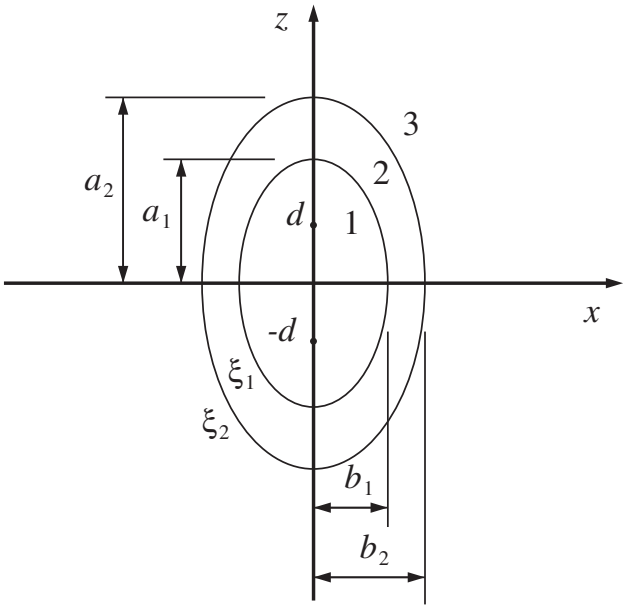

Figure 11. Cross-section of a coated spheroid.

In equation (15), ρ_{ij} is given in equation (9), P_s^t is a Legendre function of the first kind and Q_s^t a Legendre function of the second kind. ξ_1 and ξ_2 are spheroidal coordinates describing the surface of region 1 (the particle core) and the outer surface of region 2 (the layer), respectively. The prime indicates the derivative normal to the surface;

$$L_s^t(\xi_j)' \equiv \left.\frac{\mathrm{d}L_s^t(\xi)}{\mathrm{d}\xi}\right|_{\xi=\xi_j} \tag{16}$$

with L either P or Q. $\mathcal{L}_{\mathrm{st}}^{12}$ is a coefficient obtained by applying continuity conditions on the electric field at the interface between the particle core and layer,

$$\mathcal{L}_{\mathrm{st}}^{12} = \frac{1-\rho_{12}}{\rho_{12}[Q_s^t(\xi_1)/P_s^t(\xi_1)] - [Q_s^t(\xi_1)'/P_s^t(\xi_1)']}. \tag{17}$$

As quoted in equations (13) and (14), the expressions for the ϵ_{jj} are truncated forms of those given in [2], which are in fact accurate up to order λ^{14}, equivalent to the accuracy of the expression for ϵ for spherical filler particles given in equation (5). The calculations of the following section use the full form of the equations given in [2] and are accurate to order λ^{14}. Equations (13) and (14) are for prolate spheroids, with $a/b > 1$. Equations for oblate spheroids ($a/b < 1$) are obtained by replacing d with $-\mathrm{i}d$ in (13) and (14) [10].

5. Example calculations for spheroidal filler particles with a lossy core

The bulk permittivity of a composite material with coated, spheroidal filler particles whose core and layer are both lossy is shown in figures 12 and 13. The material parameters are $\epsilon_1' = \epsilon_2' = 1$, $\sigma_1 = 1.0\,\mathrm{S\,m^{-1}}$ and $\sigma_2 = 0.01\,\mathrm{S\,m^{-1}}$. The particle volume fraction, f, is 0.02, lower than in the results calculated above for spherical particles, to permit aspect ratios a/b in the range from 0.2 to 5.0. For spheroidal particles arranged on a simple-cubic lattice, with axis of rotation parallel to one of the lattice vectors, the maximum volume fraction, f_{max}, for non-overlapping particles is

$$f_{\mathrm{max}} = \begin{cases} \dfrac{\pi}{6}\left(\dfrac{b}{a}\right)^2 & \dfrac{a}{b} \geqslant 1, \\ \dfrac{\pi}{6}\left(\dfrac{a}{b}\right) & \dfrac{a}{b} \leqslant 1. \end{cases}$$

The volume fraction of the particle core, f_1, is held constant at 0.014 58, corresponding to layer thickness $t = 0.1$ when the particle aspect ratio $a/b = 1$. Note that, in this discussion, a and b refer to the semi-axis lengths of the whole filler particle, corresponding to a_2 and b_2 in figure 11.

5.1. Effect of a/b and particle orientation in the applied electric field

In figures 12 and 13, the effect of varying the particle aspect ratio, on ϵ_{xx} and ϵ_{zz}, respectively, is shown. In figure 12 the electric field is applied parallel to the x-axis, figure 11, perpendicular to the rotation axis of the spheroid, whereas in figure 13 it is applied parallel to the z-axis, parallel to the rotation axis of the spheroid. In both cases, the frequency at which the first relaxation occurs is unchanged by adjusting

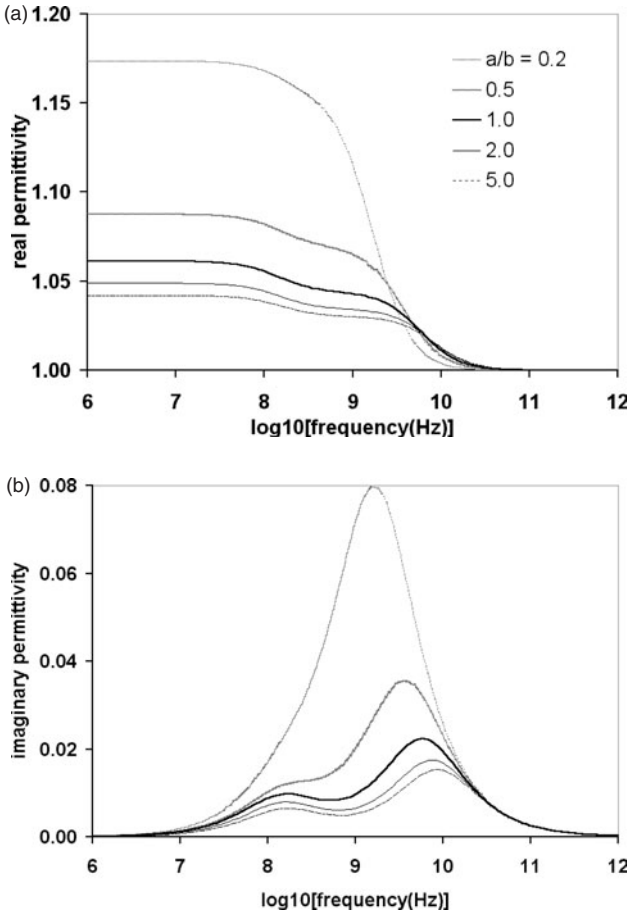

Figure 12. ϵ_{xx} as a function of ν and a/b. $\epsilon_1' = \epsilon_2' = 1$. $\sigma_1 = 1.0\,\mathrm{S\,m^{-1}}$ and $\sigma_2 = 0.01\,\mathrm{S\,m^{-1}}$. $f = 0.02$ and $f_1 = 0.014\,58$.

a/b. The frequency of the second loss process declines, and the magnitude of the loss increases, as the dimension of the particle increases in the direction parallel to the applied electric field. This means that the loss processes diverge for ϵ_{xx} as $a/b \to \infty$ and diverge for ϵ_{zz} as $a/b \to 0$.

6. Conclusions and comments

Comparing figures 4 and 5 with 6 and 7 it may be concluded that, if $\sigma_1 > \sigma_2$, there will be two loss processes whose relaxation frequencies diverge as σ_1/σ_2 increases. If σ_1 is increased, ν_2 moves to higher frequency in proportion with the change in σ_1. If σ_2 is reduced, ν_1 moves to lower frequency.

If $\sigma_1 > \sigma_2$ so that two relaxation processes are evident, then the effect of adjusting ϵ_1' and ϵ_2' can be seen from figures 8 and 9. Adjusting ϵ_1' has the effect of changing ϵ_∞ alone whereas adjusting ϵ_2' changes the value of both ϵ_i and ϵ_∞. It may be concluded that, in this case, the magnitude of the relaxation at ν_1 is strongly influenced by ϵ_2' and that at ν_2 by ϵ_1'.

Figures 12 and 13 show the effect, on the two components of the anisotropic bulk permittivity, of varying the particle aspect ratio a/b while the volume fractions of the three-phases remains constant. It is noticeable that the magnitude of the loss increases dramatically as the dimension of the particle increases in the direction parallel to the applied electric field.

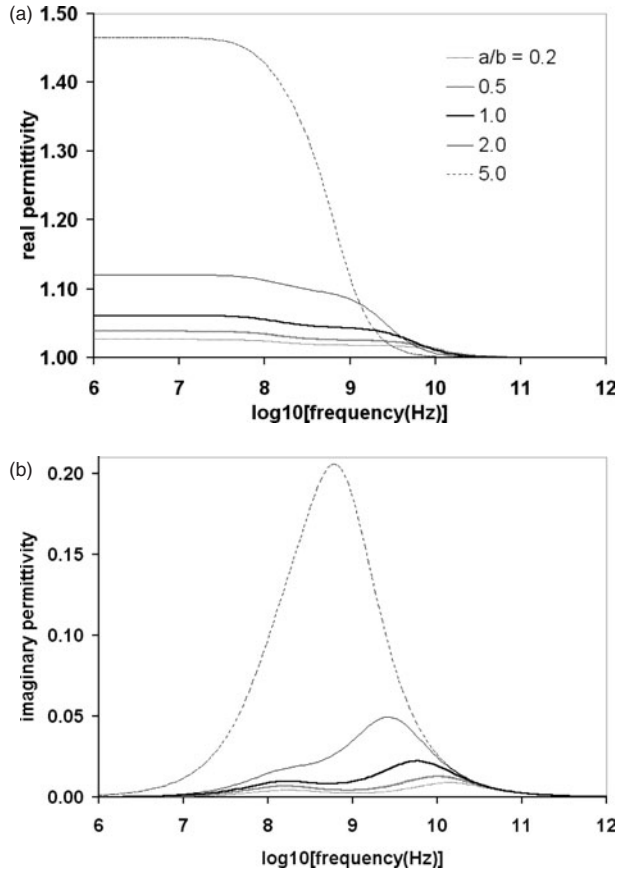

Figure 13. ϵ_{zz} as a function of ν and a/b. Other parameters are as in figure 12.

Practically speaking, it is usually the case that dispersion curves measured experimentally are broader than those predicted by theory (see, e.g. [8]). This is likely to be true due to difficulty in tightly controlling the specifications of the filler particles; their size, shape and, very importantly in this case, the thickness and uniformity of the layer. Overcoming these material challenges will permit practical exploitation of the fine features observed in the dispersion curves here.

Appendix

For a system of coated, spherical filler particles dispersed in a matrix, analytical expressions for the frequencies at which relaxation processes occur, ν_1 and ν_2, have been determined by Pauly and Schwan [1,3]. These may be written

$$2\pi\nu_1 = \frac{2T_2}{T_1 + \sqrt{T_1^2 - 4T_2T_3}}, \tag{18}$$

$$2\pi\nu_2 = \frac{T_1 + \sqrt{T_1^2 - 4T_2T_3}}{2T_3} \tag{19}$$

for $\nu_1 < \nu_2$, where the T_i are given in terms of the permittivity values of the individual phases, ϵ_j, and their volume fractions, f_j (see figure 1).

$$T_1 = [(1-f)(\epsilon_2' a + \sigma_2 c) + (2+f)(\epsilon_3' b + \sigma_3 d)]\epsilon_0, \tag{20}$$

$$T_2 = (1-f)\sigma_2 a + (2+f)\sigma_3 b, \tag{21}$$

$$T_3 = [(1-f)\epsilon_2' c + (2+f)\epsilon_3' d]\epsilon_0^2 \tag{22}$$

and

$$a = \left(1 + \frac{2f_1}{f}\right)\sigma_1 + 2\left(1 - \frac{f_1}{f}\right)\sigma_2, \tag{23}$$

$$b = \left(1 - \frac{f_1}{f}\right)\sigma_1 + \left(2 + \frac{f_1}{f}\right)\sigma_2, \tag{24}$$

$$c = \left(1 + \frac{2f_1}{f}\right)\epsilon_1' + 2\left(1 - \frac{f_1}{f}\right)\epsilon_2', \tag{25}$$

$$d = \left(1 - \frac{f_1}{f}\right)\epsilon_1' + \left(2 + \frac{f_1}{f}\right)\epsilon_2'. \tag{26}$$

$\epsilon_0 = 8.85 \times 10^{-12}\,\mathrm{F\,m^{-1}}$ is the permittivity of free space and $f = f_1 + f_2$ is the volume fraction of the whole particle.

References

[1] Pauly H and Schwan H P 1959 *Z. Naturf.* **14b** 125
[2] Harfield N 2000 *J. Mater. Sci.* **35** 5809–16
[3] Hanai T 1968 Electrical properties of emulsions *Emulsion Science* ed P Sherman (London: Academic) chapter 5
[4] Sihvola A and Lindell I V 1989 *J. Electromagnetic Waves Appl.* **3** 37–60
[5] Zuzovsky M and Brenner H 1977 *J. Appl. Math. Phys.* **28** 979–92
[6] Sangani A S and Yao C 1988 *J. Appl. Phys.* **63** 1334–41
[7] Bowler N 2003 *Phys. Rev.* B submitted
[8] Steeman P A M and Maurer F H J 1990 *Colloid Polym. Sci.* **268** 315–25
[9] Harfield N 1999 *J. Phys. D: Appl. Phys.* **32** 1104–13
[10] Morse P M and Feshbach H 1953 *Methods of Theoretical Physics* (New York: McGraw-Hill) chapter 11